Published in final edited form as:
Nature. 2009 January 15; 457(7227): 322–326. doi:10.1038/nature07526.

The insect nephrocyte is a podocyte-like cell with a filtration slit diaphragm

Helen Weavers[1,*], **Silvia Prieto-Sánchez**[2,*], **Ferdinand Grawe**[3], **Amparo Garcia-López**[4], **Ruben Artero**[4], **Michaela Wilsch-Braeuninger**[5], **Mar Ruiz-Gómez**[2], **Helen Skaer**[1], and **Barry Denholm**[1]

[1] Department of Zoology, University of Cambridge, Downing Street, Cambridge, CB2 3EJ, UK

[2] Centro de Biología Molecular Severo Ochoa, CSIC, UAM, Cantoblanco, 28049, Madrid, Spain.

[3] Institut für Genetik, Heinrich-Heine-Universität, Düsseldorf, D-40225, Germany

[4] Department of Genetics, University of Valencia, Burjasot, Valencia 46100, Spain

[5] Max Planck Institute of Molecular Cell Biology and Genetics, Dresden, Germany

Abstract

The nephron is the basic structural and functional unit of the vertebrate kidney. It is composed of a glomerulus, the site of ultrafiltration, and a renal tubule, along which the filtrate is modified. Although widely regarded as a vertebrate adaptation1 'nephron-like' features can be found in the excretory systems of many invertebrates, raising the possibility that components of the vertebrate excretory system were inherited from their invertebrate ancestors2. Here we show that the insect nephrocyte has remarkable anatomical, molecular and functional similarity with the glomerular podocyte, a cell in the vertebrate kidney that forms the main size-selective barrier as blood is ultrafiltered to make urine. In particular, both cell types possess a specialised filtration diaphragm, known as the slit diaphragm in podocytes or the nephrocyte diaphragm in nephrocytes. We find that fly orthologues of the major constituents of the slit diaphragm, including nephrin, neph1, CD2AP, ZO-1 and podocin are expressed in the nephrocyte and form a complex of interacting proteins that closely mirrors the vertebrate slit diaphragm complex. Furthermore, we find the nephrocyte diaphragm is completely lost in flies mutant for nephrin or neph1 orthologues, a phenotype resembling loss of the slit diaphragm in the absence of either nephrin (as in the human kidney disease NPHS1) or neph1. These changes drastically impair filtration function in the nephrocyte. The similarities we describe between invertebrate nephrocytes and vertebrate podocytes provide evidence suggesting the two cell types are evolutionarily related and establish the nephrocyte as a simple model in which to study podocyte biology and podocyte-associated diseases.

Filtration of blood in the vertebrate kidney occurs within the glomerulus of the nephron (Fig 1a,b). The filtration barrier is formed by podocytes, specialised epithelial cells, which send out interdigitating foot processes to enwrap the glomerular capillaries. These processes are separated by 30-50nm wide slit pores spanned by the slit diaphragm3,4, which together with the glomerular basement membrane (GBM), form a size- and charge-selective filtration

Author for correspondence: hs17@cam.ac.uk.
* these authors contributed equally to this work

Author contribution

B.D., H.S., M.R-G. designed and directed the project. B.D., H.W., M.R-G. and S.P-S. performed the experiments. F.G. and M.W-B. provided invaluable technical assistance. A.G-L. and R.A. provided materials. B.D. and H.S. wrote the paper. All authors discussed results and commented on the manuscript.

Europe PMC Funders Author Manuscripts

barrier (Fig. 1b). Disruption to this barrier in disease leads to leakage of blood proteins into the urinary space and to kidney failure5.

Although invertebrate excretory systems are considered to lack nephrons, 'nephron-like' components, such as filtration cells and ducts in which the filtrate is modified, are widespread (Fig. 1c)6,7. Insect nephrocytes regulate haemolymph composition by filtration, followed by endocytosis and processing to sequester and/or secondarily metabolise toxic materials7-9. *Drosophila* has two types – garland and pericardial nephrocytes (Fig. 1e-g). They are tethered to the oesophagus (Fig. 1g, 3g) or heart (Fig. 1f), and are bathed in haemolymph. Extensive infolding of the plasma membrane generates a network of labyrinthine channels or lacunae flanked by nephrocyte foot processes (Fig. 1h). The channel entrances are narrow slits 30nm in width, spanned by a single or double filament forming a specialised filtration junction; the nephrocyte diaphragm (Fig. 1h,i and Fig. 3c). Each nephrocyte is enveloped by basement membrane (Fig. 1h and Fig. 3c). The nephrocyte diaphragm and basement membrane behave as a size and charge-selective barrier7,9 (Fig. 1d) and filtrate is endocytosed from the sides of the lacunae. Thus the anatomy of the nephrocyte and podocyte filtration barriers are remarkably similar3.

In view of this similarity we investigated whether the nephrocyte diaphragm is molecularly related to the slit diaphragm. The major slit diaphragm components, the transmembrane Ig-domain superfamily proteins nephrin and neph1 are co-expressed in the podocyte and interact across the slit pore by homo- and hetero-typic binding to form the diaphragm4,10-16. Mutations in nephrin, as in human congenital nephrotic syndrome of the Finnish type (NPHS1)10, or in neph17, cause slit diaphragm loss and foot process effacement, resulting in breakdown of the filtration barrier and proteinuria.

Drosophila has two nephrin orthologues – *sticks and stones* (*sns*) and *hibris* (*hbs*) and two neph1 orthologues – *dumbfounded (duf*) and *roughest* (*rst*) (Supplementary Table 1). As *hbs* and *rst* are expressed in only a subset of nephrocytes (data not shown), we focus on *sns* and *duf*. Sns and Duf are expressed throughout life in both nephrocyte types (Figs. 2a-g, adult data not shown), from midembryogenesis for garland cells (Supplementary Fig.1 and Fig. 2a,b) and from the first larval instar for pericardial cells (Fig. 2c). Interestingly, the onset of Sns and Duf expression correlates in time with the appearance of the nephrocyte diaphragm at the ultrastructural level18,19. Both proteins localise to the plasma membrane (Fig. 2d-g) and double labelling reveals precise co-localisation (Fig. 2h). This finding is initially surprising because in most contexts Sns and Duf are expressed in complementary patterns and mediate interaction between cells of different type. The only other situation where the two types of Ig-domain proteins are co-expressed in the same cell is the vertebrate podocyte14. We find that Sns and Duf are dependent on one another for stabilization at the plasma membrane. Loss or knockdown of either protein in embryonic (Fig 2i-l) or larval (Fig 2m-p) nephrocytes leads to a loss, severe reduction or mislocalisation of the other. These data demonstrate an essential interaction between the two proteins in the same cell, similar to those between nephrin and neph1 in the podocyte13-16. The precise subcellular location of the proteins was revealed by immuno-electron microscopy. Both Sns and Duf specifically localise to the nephrocyte diaphragm (Fig 2q-s) and double labelling reveals close colocalisation between the two proteins (Fig. 2t,u).

Garland and pericardial nephrocytes are correctly specified in *sns* and *duf* mutants (Supplementary Fig. 2a-k). However, given the importance of the Ig-domain proteins in slit diaphragm formation, we examined the ultrastructure of the diaphragm in *sns* and *duf* mutants. In wild-type garland cells, nephrocyte diaphragms and associated lacunae appear during mid-embryogenesis (Supplementary Fig. 2l), progressively increasing in number (Fig. 1h). Diaphragms densely populate the cell periphery in third instar larvae (Fig. 3c).

Strikingly, *sns* or *duf* mutant garland cells completely lack nephrocyte diaphragms at every stage and lacunae are rarely detected (cf Fig. 3a,b with Fig.1i, Fig 3c with d, Supplementary Fig. 2m,n with l). Occasional infoldings do form, but are never bridged by diaphragms (Fig. 3b, Supplementary Fig. 2n). Instead, the nephrocyte surface contains frequent, small patches of electron-dense subcortical material (Fig. 3a^{i}); possible remnants of undercoat normally associated with the wild-type diaphragm. These observations suggest that in the absence of the diaphragm, foot processes are unstable and undergo effacement. Scanning electron microscopy reveals the surface smoothening in mutant garland cells (cf Fig. 3e and f). These phenotypes are remarkably similar to those of podocytes lacking nephrin or neph15,17. Thus, by analogy with nephrin and neph1 in the slit diaphragm, we suggest that Sns and Duf interact through their extracellular domains to form the nephrocyte diaphragm itself.

We noted that the basement membrane in *sns* knockdown and *duf* larval nephrocytes was irregular and dramatically expanded (cf Fig. 3c,d). The basement membrane in *duf* nephrocytes has an average depth of 202nm (± 24, n=13) compared with 57nm (± 4, n=11) for wild-type. This results from an increase in deposition of the *Drosophila* collagen IV (Viking) (Fig. 3g,h, Supplementary Fig. 3). However this is unlikely to account for the four-fold thickening observed, and we suggest that a further contributing factor is accumulation of haemolymph proteins that clog the basement membrane due to inefficient filtration.

Given the similarities between the morphology and molecular requirements for podocyte and nephrocyte diaphragms, we tested the ability of human nephrin to rescue the *sns* mutant phenotype. However nephrocytes are sensitive to absolute levels of *sns*, so that even moderate overexpression produced abnormal phenotypes. We therefore compared the effects of overexpressing *Drosophila sns* with human nephrin. Resulting phenotypes are strikingly similar, including abnormal nephrocyte foot process morphology and marked thickening of diaphragm filaments (Fig. 3i,j). These data indicate that precise levels of Sns are critical for diaphragm formation and more importantly that human nephrin and *Drosophila* Sns function in equivalent ways.

Vertebrate nephrin and neph1 form a multi-protein complex at the slit diaphragm with zonula occludens-1 (ZO-1)20, CD2AP21,22 and podocin23 (Supplementary Table 1). Mutations in these genes result in kidney disease21,23,24. We asked whether the fly orthologues (Supplementary Table 1) contribute to the nephrocyte diaphragm. *in situ* hybridisation reveals that *pyd* (ZO-1), *CG31012* (CD2AP) and *Mec2* (NPHS2/podicin, Supplementary Fig. 4) are expressed in nephrocytes (Fig. 4a-f). Furthermore, Pyd-GFP precisely co-localises with Duf to the membrane (Fig. 4g), mirroring co-localisation of ZO-1 and neph1 in the podocyte20.

Molecular interactions between these vertebrate slit diaphragm-associated proteins have been established (Fig. 4h, black arrows)11,20,22,25. To test whether fly orthologues form a similar complex, we performed a yeast two-hybrid analysis with Sns and Duf intracellular domains (Fig. 4i). Sns interacts with Mec-2 (podocin) and Duf interacts with Pyd (ZO-1) (Fig. 4j). Interaction between Duf and Pyd was independently confirmed by co-immunoprecipitation (Fig. 4k). A previous report established direct association between Sns and Duf26. These interactions between the fly proteins (Fig. 4h, red arrows) closely resemble those described for slit diaphragm-associated proteins (Fig. 4h, black arrows). These data, taken together with those described above, provide strong evidence that the nephrocyte diaphragm (Fig. 4l) and slit diaphragm are molecularly homologous structures.

Insect nephrocytes are size and charge-selective in their sequestration of materials from the haemolymph. Selectivity is based on the characteristics of the diaphragm and basement membrane, which act together as a filtration barrier7,9. To test filtration capacity of the

Drosophila nephrocyte diaphragm we assayed the passage of fluorescently-labelled dextrans of different sizes. If the nephrocyte diaphragm acts as a size-selective filter we reasoned that, like the vertebrate slit diaphragm27, it would allow free passage of small (10,000mw) but exclude large (500,000mw) dextrans (Fig. 5b). In agreement with our expectations, uptake of the 500,000mw dextran in wild-type nephrocytes is significantly lower than the 10,000mw dextran (1:3.6 n=20; Fig. 5a,f). These data strongly suggest that the nephrocyte diaphragm functions as a size-based filtration diaphragm (endocytosis from foot process tips could account for low levels of large dextran uptake, Fig. 5b). We anticipated higher uptake of the large dextran in Ig-domain mutant nephrocytes because they lack diaphragms. However, while the level of uptake of the small dextran in *duf* or *sns* nephrocytes is unaltered compared to wild-type, we find a dramatic reduction in large dextran uptake (Fig. 5c,d,f); large to small ratio is 1:22.5 (n = 20) for *duf* and 1:15.3 (n = 19) for *sns*. Instead, the large dextran appears as a halo surrounding the cell (Fig. 5c,d). The thickening of basement membrane observed in *duf* nephrocytes (Fig. 3d) could explain the exclusion of large dextran (Fig. 5e). This highlights a further parallel between nephrocytes and podocytes. An endocytosis-based clearance mechanism in podocytes prevents clogging of the GBM with blood plasma proteins; the slit-diaphragm associated protein CD2AP has been implicated in this process24,28. We suggest that an equivalent clearance mechanism exists in nephrocytes and that this mechanism requires Sns and Duf function.

Whatever the causes of reduction in filtration capability, the animal's haemolymph physiology will be disturbed. We tested this hypothesis by feeding larvae silver nitrate, a toxin endocytosed and concentrated in nephrocytes (Fig. 5h). At low concentrations of silver nitrate, viability of control larvae is not compromised (82% eclose as adults, Fig. 5i) but *duf* larvae show a greatly reduced viability (26% eclose, Fig. 5i). A previous study showed a requirement for nephrocytes in the face of toxic stress29. Our data show that Ig-domain proteins are essential for this function.

We have highlighted similarities between podocytes and nephrocytes but podocytes are an integral part of the nephron (Fig. 1a), whereas the nephrocyte is spatially separated from its renal (Malpighian) tubule (Fig. 1c). Such differences have contributed to the traditional view that vertebrate and invertebrate excretory systems are unrelated1. Nevertheless, nephron-like features are present in the excretory systems of a wide variety of invertebrates and in the protochordate *Amphioxus*, suggesting a common origin2. The molecular parallels between nephrocytes and podocytes described here support this hypothesis, and it will be of interest to determine whether nephrin/neph-like protein complexes are found in other invertebrate filtration diaphragms.

Defects in the slit diaphragm complex underlie human diseases whose unifying feature is proteinurea and kidney failure. These symptoms result from defective filtration, but in addition the nephrin/neph1 complex regulates podocyte behaviours such as cell survival, polarity, actin dynamics and endocytosis30. How these functions of the slit diaphragm relate to disease pathologies is presently unclear. The fly nephrocyte also depends on the activity of a nephrin/neph1 complex for survival, shape and selective endocytosis and thus provides a simple and genetically tractable model in which the multiple roles of the slit diaphragm complex can be addressed.

METHODS SUMMARY

Fly strains

Flies were reared on standard food at room temperature, 18°C or 25°C. The strains used are listed in the Methods.

Nephrocyte filtration assay

Garland cells were dissected, incubated with AlexaFluor568-Dextran (10,000mw) and Fluorescein-Dextran (500,000mw) (Molecular probes) at a concentration of 0.33mg/ml at 25°C for 5 minutes, washed on ice, fixed and mounted. Dextran uptake was quantified by counting pixel number exceeding background threshold using Volocity software.

Toxin stress assay

First instar larvae of the appropriate genotype were transferred to agar-only plates supplemented with yeast paste or with yeast paste containing $AgNO_3$ (2g yeast in 3.5ml of 0.003% $AgNO_3$), and allowed to develop at 25°C. Percentage of eclosing adults was scored.

Antibodies

Antibodies used were: anti-Sns (1:200, S.Abmayr), anti-Kirre (1:200, K. Fischbach), anti-Duf extracellular (1:50, M.R-G.), anti-Duf intracellular (1:500, M.R-G.), anti-βgal (1:1000, ICN Biomedicals), anti-HRP (1:200, Jackson ImmunoResearch), anti-Pericardin (1:2, DSHB), anti-GFP (1:500, Invitrogen Molecular probes).

Confocal and electron microscopy

Confocal and electron microscopy was carried out using standard techniques. For immuno-electron microscopy, dissected larval garland cells were fixed in 4% formaldehyde + 0.05% glutaraldehyde, embedded in gelatin, cryosectioned and incubated with anti-Duf extracellular (1:5), anti-Kirre (1:20), or anti-Sns (1:20) followed by 5nm and 10nm gold-conjugated secondary antibody.

Yeast two-hybrid

The intracellular domains of Sns and Duf were tested for interaction with: Pyd (isoform f); CD2AP (SD08724); C-terminal cytoplasmic domain of Mec2 using the Clontech Matchmaker GAL4 two-hybrid system. Interaction was indicated by growth in absence of histidine. 5mM 3′AT (Sigma) was included to titrate residual auto-activation from the bait fusion proteins.

Co-immunoprecipitation experiments

Drosophila S2 cells transiently co-transfected with pMK33/pMtHy-duf and pAC5.1V5-His-pyd were induced for 20 hours with 0.7mM $CuSO_4$. Total cell lysate was split and each half immunoprecipitated with either anti-V5 or anti-Duf intracellular and probed with anti-Duf intracellular and anti-V5 following standard protocols.

METHODS

Fly strains

The following fly genotypes were used: OregonR (wild-type strain); sns^{XB3} and *UAS-sns* (gift from S. Abmayr); for embryonic analysis of *duf* $Df(1)w^{67k30}$ hemizygotes were used; for larval analysis of *duf* $Df(1)w^{67k30}/Df(1)N^{5419}$ transheterozygous or $Df(1)duf^{sps-1}$ [small deficiency removing the *duf* locus only, a description of this allele will published elsewhere (Prieto-Sánchez et al., in preparation)] were used; *rP298* (*duf-LacZ*); *UAS-Pyd-GFP* (gift from M. Affolter); *Viking-GFP* (gift from L.Cooley); *UAS-sns-RNAi* (a 1047bp fragment was obtained by PCR from *sns* cDNA using primers 5′-CCAGTTCGTATAATGACACCG and 5′-CCTACAGCTATACGAGGTGTC and used to make intron-spliced hairpin RNA according to31; *UAS-nephrin* [human NPHS1 cDNA (gift from K. Tryggvason) cloned into pUAST]; *G447.2-GAL4* (embryonic garland cell driver; gift from R. Reuter); *Prospero-Gal4*

(larval garland cell driver; gift from Chris Doe). Fly crosses were maintained at 25°C except for the overexpression experiment when animals were maintained at 29°C to ensure maximum transgene expression. Marked balancer chromosomes (Kr-Gal4, UAS-GFP) and/or PCR-genotyping32 from carcasses remaining after dissection were used to identify appropriate genotypes.

Nephrocyte filtration assay

Garland nephrocytes (including a small portion of oesophagus and the proventriculus) were dissected from third instar larvae in Shields and Sang medium (Sigma), then transferred to media containing AlexaFluor568-Dextran (10,000mw) and Fluorescein-Dextran (500,000mw) (Molecular probes) at a concentration of 0.33mg/ml and incubated at 25°C for 5 minutes. The cells were washed on ice for 10 minutes in cold PBS, fixed in 4% formaldehyde for 10 minutes at room temperature, rinsed once in PBS and then mounted in vectashield (Vectorlabs). All post-dissection procedures were carried out in the dark. A single confocal section of the cell midpoint was taken using a Leica SP1 confocal microscope and dextran uptake was quantified by counting pixel number exceeding background threshold within the sample area (typically the whole cell) using Volocity software. Average fluorescence from the proventriculus epithelium (where dextran uptake does not occur) was used to set the background threshold. The same threshold was used for all experiments. Control cells incubated with Dextran on ice showed no uptake.

Toxin stress assay

Flies of the appropriate genotype were allowed to lay on standard apple juice plates supplemented with yeast. After approximately 24 hours, freshly emerging first instar larvae from this plate were transferred to agar-only plates supplemented with yeast paste or with yeast paste containing $AgNO_3$ (2g yeast in 3.5ml of 0.003% $AgNO_3$), and allowed to develop at 25°C. Percentage of eclosing adults was scored.

In situ hybridisation and immunohistochemistry

Whole mount in situ hybridization and immunohistochemistry to embryos and third instar nephrocytes were carried out using standard techniques. Antibodies used: anti-Sns (1:200, gift from S. Abmayr), anti-Kirre (1:200, gift from K. Fischbach), anti-Duf extracellular (1:50), anti-Duf intracellular (1:500, the generation of both antisera will be publish elsewhere), anti-βgal (1:1000, ICN Biomedicals), anti-HRP (1:200, Jackson ImmunoResearch), anti-Pericardin (1:2, DSHB), anti-GFP (1:500, Invitrogen Molecular probes), AlexaFluor 488 phalloidin and AlexaFluor 568 phalloidin (1:20, Invitrogen Molecular probes), TOTO3 and TO-PRO-3 (1:100, Invitrogen Molecular probes).

Confocal and electron microscopy

Confocal microscopy, TEM and SEM were carried out using standard techniques. For immuno-electron microscopy, dissected garland cells were fixed in 4% formaldehyde + 0.05% glutaraldehyde, embedded in gelatin, cryosectioned and incubated with anti-Duf extracellular (1:5), anti-Kirre (1:20), or anti-Sns (1:20) followed by 5nm and 10nm gold-conjugated secondary antibody. In some cases confocal images correspond to *z*-projections from a series of confocal sections.

Collagenase treatment

Third instar garland cells were incubated in 0.1% collagenase type I in PBS for three minutes at 37°C.

Yeast two-hybrid

The intracellular domains of Sns and Duf were used as bait (cloned into pGBKT7, Clontech) and tested for interaction with: Pyd (isoform f); CD2AP (SD08724); C-terminal cytoplasmic domain of Mec2 (all cloned into pGADT7, Clontech). Interaction was indicated by growth in absence of histidine. 5mM 3′AT (Sigma) was included to titrate residual auto-activation from the bait fusion proteins.

Co-immunoprecipitation experiments

Drosophila S2 cells transiently co-transfected with pMK33/pMtHy-duf and pAC5.1V5-His-pyd were induced for 20 hours with 0.7mM $CuSO_4$. Total cell lysate was split and each half immunoprecipitated with either anti-V5 or anti-Duf and probed consecutively with anti-Duf and anti-V5 or anti-V5 and anti-Duf, respectively, following standard protocols.

Supplementary Material

Refer to Web version on PubMed Central for supplementary material.

Acknowledgments

Felix Evers, Zoltan Cseresnyes and Milagros Guerra for technical assistance. Susan Abmayr, Lynn Cooley, Chris Doe, Markus Affolter, Karl Fischbach and Karl Tryggvason for reagents. We thank Maneesha Inamdar, Adrian Woolf, Irene Miguel-Aliaga, Felix Evers, Matthias Landgraf and members of the Skaer lab for helpful discussions and Elisabeth Knust and Wieland B. Huttner for their generous support. This work was supported by Wellcome Trust grants awarded to H.S. (072441 and 079221, H.W., B.D., H.S.); Deutsche Forschungsgemeinschaft (SFB 590) awarded to Elisabeth Knust (F.G.), ARC 1242 (H.W., B.D., H.S., F.G.); MEC grant awarded to M.R-G. (BFU2007-62201, S.P-S., M.R-G.); Fundación Ramón Areces grant to the CBMSO (M.R-G.); EC grant LSHG-CT-2004-511978 to MYORES (M.R-G.); an FPU fellowship from the MEC awarded to A.G-L.

References

1. Smith, HW. From Fish to Philosopher. Little, Brown; Boston: 1953.
2. Ruppert EE. Evolutionary Origin of the Vertebrate Nepron. American Zoologist. 1994; 34:542–533.
3. Rodewald R, Karnovsky MJ. Porous substructure of the glomerular slit diaphragm in the rat and mouse. J Cell Biol. 1974; 60:423–33. [PubMed: 4204974]
4. Wartiovaara J, et al. Nephrin strands contribute to a porous slit diaphragm scaffold as revealed by electron tomography. J Clin Invest. 2004; 114:1475–83. [PubMed: 15545998]
5. Patrakka J, et al. Congenital nephrotic syndrome (NPHS1): features resulting from different mutations in Finnish patients. Kidney Int. 2000; 58:972–80. [PubMed: 10972661]
6. Berridge, MJ.; Oschman, JL. Transporting Epithelia. Academic Press; New York: 1972.
7. Crossley, AC. Comprehensive Insect Physiology, Biochemistry and Pharmacology. Kerkut, GA.; Gilbert, LI., editors. Pergamon Press; Oxford: 1985. p. 487-515.
8. Kowalevsky A. Ein Beitrag zur Kenntnis der Excretions-organe. Biol. Centralbl. 1889; 9:74–79.
9. Locke, M.; Russell, VW. Microscopic Anatomy of Invertebrates. Harrison, FW.; Locke, M., editors. Wiley; 1998. p. 687-709.
10. Kestila M, et al. Positionally cloned gene for a novel glomerular protein--nephrin--is mutated in congenital nephrotic syndrome. Mol Cell. 1998; 1:575–82. [PubMed: 9660941]
11. Sellin L, et al. NEPH1 defines a novel family of podocin interacting proteins. Faseb J. 2003; 17:115–7. [PubMed: 12424224]
12. Ruotsalainen V, et al. Nephrin is specifically located at the slit diaphragm of glomerular podocytes. Proc Natl Acad Sci U S A. 1999; 96:7962–7. [PubMed: 10393930]
13. Gerke P, Huber TB, Sellin L, Benzing T, Walz G. Homodimerization and heterodimerization of the glomerular podocyte proteins nephrin and NEPH1. J Am Soc Nephrol. 2003; 14:918–26. [PubMed: 12660326]

14. Barletta GM, Kovari IA, Verma RK, Kerjaschki D, Holzman LB. Nephrin and Neph1 co-localize at the podocyte foot process intercellular junction and form cis hetero-oligomers. J Biol Chem. 2003; 278:19266–71. [PubMed: 12646566]
15. Khoshnoodi J, et al. Nephrin promotes cell-cell adhesion through homophilic interactions. Am J Pathol. 2003; 163:2337–46. [PubMed: 14633607]
16. Liu G, et al. Neph1 and nephrin interaction in the slit diaphragm is an important determinant of glomerular permeability. J Clin Invest. 2003; 112:209–21. [PubMed: 12865409]
17. Donoviel DB, et al. Proteinuria and perinatal lethality in mice lacking NEPH1, a novel protein with homology to NEPHRIN. Mol Cell Biol. 2001; 21:4829–36. [PubMed: 11416156]
18. Tepass U, Hartenstein V. The development of cellular junctions in the Drosophila embryo. Dev Biol. 1994; 161:563–96. [PubMed: 8314002]
19. Rugendorff A, Younossi-Hartenstein A, Hartenstein V. Embryonic origin and differentiation of the Drosophila heart. Roux's Archive of Developmental Biology. 1994:266–280.
20. Huber TB, et al. The carboxyl terminus of Neph family members binds to the PDZ domain protein zonula occludens-1. J Biol Chem. 2003; 278:13417–21. [PubMed: 12578837]
21. Shih NY, et al. Congenital nephrotic syndrome in mice lacking CD2-associated protein. Science. 1999; 286:312–5. [PubMed: 10514378]
22. Shih NY, et al. CD2AP localizes to the slit diaphragm and binds to nephrin via a novel C-terminal domain. Am J Pathol. 2001; 159:2303–8. [PubMed: 11733379]
23. Boute N, et al. NPHS2, encoding the glomerular protein podocin, is mutated in autosomal recessive steroid-resistant nephrotic syndrome. Nat Genet. 2000; 24:349–54. [PubMed: 10742096]
24. Kim JM, et al. CD2-associated protein haploinsufficiency is linked to glomerular disease susceptibility. Science. 2003; 300:1298–300. [PubMed: 12764198]
25. Schwarz K, et al. Podocin, a raft-associated component of the glomerular slit diaphragm, interacts with CD2AP and nephrin. J Clin Invest. 2001; 108:1621–9. [PubMed: 11733557]
26. Galletta BJ, Chakravarti M, Banerjee R, Abmayr SM. SNS: Adhesive properties, localization requirements and ectodomain dependence in S2 cells and embryonic myoblasts. Mech Dev. 2004; 121:1455–68. [PubMed: 15511638]
27. Kramer-Zucker AG, Wiessner S, Jensen AM, Drummond IA. Organization of the pronephric filtration apparatus in zebrafish requires Nephrin, Podocin and the FERM domain protein Mosaic eyes. Dev Biol. 2005; 285:316–29. [PubMed: 16102746]
28. Akilesh S, et al. Podocytes use FcRn to clear IgG from the glomerular basement membrane. Proc Natl Acad Sci U S A. 2008; 105:967–72. [PubMed: 18198272]
29. Das D, Aradhya R, Ashoka D, Inamdar M. Post-embryonic pericardial cells of Drosophila are required for overcoming toxic stress but not for cardiac function or adult development. Cell Tissue Res. 2008; 331:565–70. [PubMed: 17987318]
30. Huber TB, Benzing T. The slit diaphragm: a signaling platform to regulate podocyte function. Curr Opin Nephrol Hypertens. 2005; 14:211–6. [PubMed: 15821412]
31. Nagel AC, Maier D, Preiss A. Green fluorescent protein as a convenient and versatile marker for studies on functional genomics in Drosophila. Dev Genes Evol. 2002; 212:93–8. [PubMed: 11914941]
32. Strunkelnberg M, et al. rst and its paralogue kirre act redundantly during embryonic muscle development in Drosophila. Development. 2001; 128:4229–39. [PubMed: 11684659]

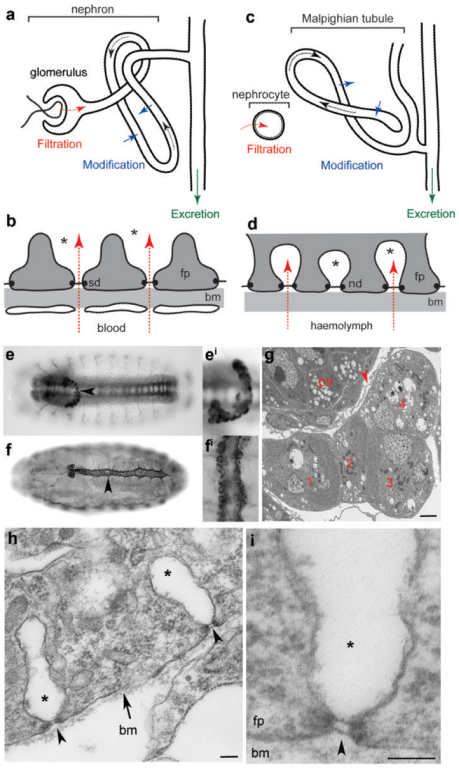

Figure 1. The glomerular and nephrocyte filtration barriers are anatomically similar

a-d, Schematic drawings of the vertebrate nephron (a), glomerular filtration barrier (b), insect excretory system (c) and nephrocyte filtration barrier (d). Ultrafiltration (red arrow), filtrate flow (black arrow) and urinary space (b) or extracellular lacunae (d) (asterisk) are shown. e,f, *Drosophila* garland (anti-HRP, e) and pericardial (anti-Pericardin, f) nephrocytes. Higher magnification images are shown in e^{i} and f^{i}. g-i, TEMs of stage 16 embryonic garland nephrocytes. g, Four garland nephrocytes surrounding the proventiculus (pv), connective fibres (arrowhead). h and i, High magnification of garland nephrocyte cell surface (h) and nephrocyte diaphragm (i) showing nephrocyte diaphragm (arrowhead), extracellular lacunae (asterisk). Scale bars 2μm (g), 100nm (h,i). fp, foot process; sd, slit diaphragm; nd, nephrocyte diaphragm; bm, basement membrane.

Europe PMC Funders Author Manuscripts

Europe PMC Funders Author Manuscripts

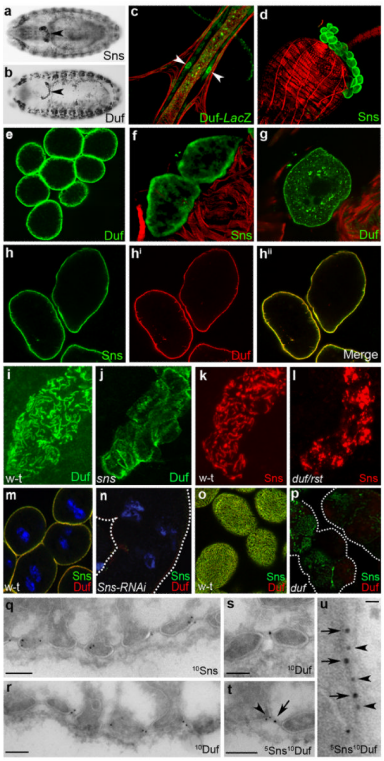

Figure 2. Sns and Duf are expressed in *Drosophila* nephrocytes

a-h, Sns (a,d,f,h) and Duf (b,c,e,g,h) expression in garland (a,b,d,e) and pericardial (c,f,g,h) nephrocytes. Embryonic (a,b, arrowheads), first instar larva (c, green, arrowheads), and third instar larvae (d-h, green). The actin cytoskeleton has been counterstained in c,d,f,g (red). h, Sns (h, green) and Duf (h^{i}, red) co-localise (h^{ii}, yellow). i-l, Clusters of ~6-8 wild-type (i,k), *sns* (j) or *duf,rst* (l) embryonic garland cells stained with anti-Duf (i,j) or anti-Sns (k,l). m-p, wild-type (m,o), *sns-RNAi* (n) and *duf* (p) third instar garland cells stained for anti-Duf (red) and anti-Sns (green) (merge appears yellow) and DNA (blue). Single optical section (m,n) or *z*-projection of cell surface (o,p) are shown. q-u, TEMs of wild-type third instar garland cells immunogold-stained for anti-Sns (q), anti-Duf (r,s) or double labelled (t,u). For double labelling 5nm (arrowhead) and 10nm (arrow) gold particles are used for Sns and Duf respectively. Scale bars 100nm (q-t) and 10nm (u).

Europe PMC Funders Author Manuscripts

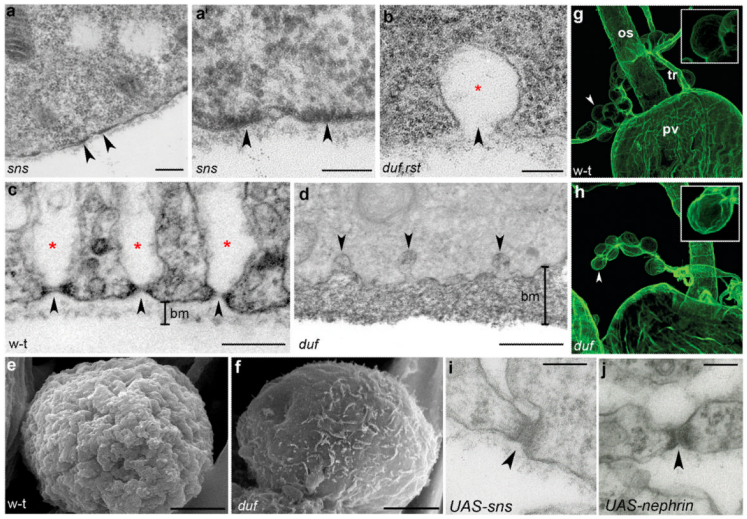

Figure 3. Sns and Duf are required for nephrocyte diaphragm formation and normal morphology

a,b, *sns* (a, a^{i}) and *duf,rst* (b) embryonic garland cells lack diaphragms and lacunae. a^{i}, higher magnification of a, showing electron-dense subcortical material (arrowheads). Small lacunae (asterisk) lacking diaphragms are occasionally found (b, arrowhead). c,d, Wild-type (c) and *duf* (d) third instar garland cells. c, diaphragms (arrowheads) and lacunae (asterisk) densely populate the nephrocyte surface. d, *duf* nephrocytes have small lacunae (arrowheads) lacking diaphragms and a substantially thickened basement membrane (bm). e,f, SEMs of wild-type (e) and *duf* (f) third instar garland nephrocytes stripped of basement membrane by collagenase treatment. *duf* nephrocytes lack the furrows corresponding to diaphragm rows. g,h, Wild-type (g) and *duf* (h) Viking-GFP (collagen IV) third instar garland cells, stained with anti-GFP (green) showing greater Viking deposition around *duf* nephrocytes (arrowheads and inset). Garland cell number is also reduced in *duf* larvae, suggesting that mutant cells ultimately die. i,j, Diaphragm and foot process morphology are abnormal (arrowheads) in *sns* (i) and human nephrin (j) embryonic overexpression. Scale bars 200nm (a,c,d), 100nm (a^{i},b), 50nm (i-j), 5μm (e,f). os, oesophagus, pv, proventriculus, tr, trachea.

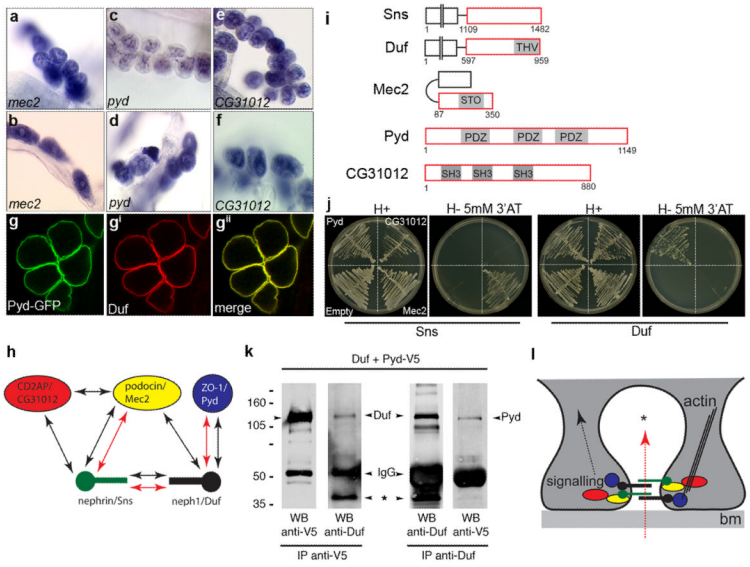

Figure 4. Analysis of slit diaphragm-associated protein orthologues in the fly nephrocyte

a-f, Third instar garland (a,c,e) and pericardial (b,d,f) nephrocytes hybridised with probes directed against *Mec2* (a,b), *pyd* (c,d) and *CG31012* (e,f). g, Pyd (g, green) and Duf (g^{i}, red) co-localise (g^{ii}, yellow) in third instar garland nephrocytes. h, Schematic drawing of the major components of the podocyte slit diaphragm (black arrows) and nephrocyte diaphragm (described here and elsewhere, red arrows). i, Schematic drawing of *Drosophila* orthologues of slit diaphragm-associated proteins: PDZ-binding domain (THV), PDZ domain (PDZ), stomatin domain (STO) and SH3 domain (SH3). Region of the protein used in the yeast two-hybrid analysis is outlined in red. j, Yeast two-hybrid analysis of Sns or Duf with Pyd, CG31012, Mec2 and negative control (empty vector). Direct protein interaction is indicated by growth of yeast on selective media (H- 5mM 3′AT). k, Duf and Pyd-V5 coimmunoprecipitate with one another from *Drosophila* cells (unlabelled arrowhead on left corresponds to Pyd, asterisk indicates cleaved form of Duf that is also coimmunoprecipitated with Pyd). l, Schematic drawing of molecular interactions at the nephrocyte diaphragm, Sns (green), Duf (black), Mec2 (yellow), Pyd (blue), CG31012 (red), direction of filtration (red arrow), extracellular lacuna (asterisk). Putative links to signalling or the actin cytoskeleton based on analogy with the equivalent complex at the slit diaphragm are shown. bm, basement membrane.

Europe PMC Funders Author Manuscripts

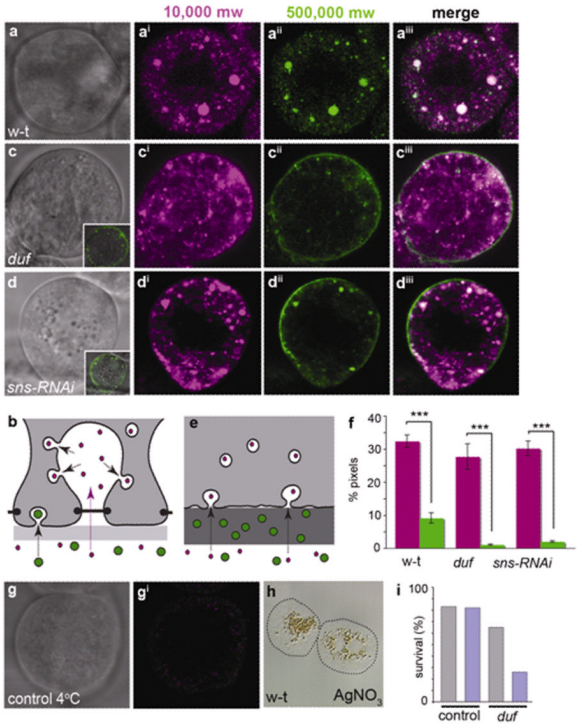

Figure 5. Sns and Duf are required for nephrocyte filtration

a,c,d, Third instar garland nephrocytes from wild-type (a), *duf* (c) and *sns RNAi* knockdown (d) animals co-incubated with 10,000mw (magenta) and 500,000mw (green) fluorescently-labelled dextran. Inset in c,d shows merged image of transmitted light and 500,000mw channels. b,e, Schematic drawing of filtration and endocytosis in wildtype (b) and *sns* or *duf* mutant (e) nephrocytes. f, Quantification of small (magenta) and large (green) dextran uptake in wild-type, *duf* and *sns RNAi* knockdown garland cells. Pixel number exceeding threshold is shown on Y-axis (error bars, S.E.M). nb, the molar ratio of dye:dextran is 1:1 (for 10,000mw) and 64:1 (for 500,000mw). g, control nephrocyte incubated with fluorescent dextran at 4°C showing no uptake (g^{i}). h, 10μm section of garland nephrocytes from a wild-type larva fed with $AgNO_3$ (brown granular staining). i, Percentage of eclosing sibling control or *duf* adults fed yeast paste (grey) or yeast paste with $AgNO_3$ (blue) (n = 65, 68, 55 and 57).

Europe PMC Funders Author Manuscripts